Modeling the optical constants of GaP, InP, and InAs

Aleksandra B. Djurišić
Department of Electrical and Electronic Engineering, University of Hong Kong, Pokfulam Road, Hong Kong

Aleksandar D. Rakić
Department of Computer Science and Electrical Engineering, The University of Queensland, Brisbane Old 4072, Australia

Paul C. K. Kwok and E. Herbert Li[a)]
Department of Electrical and Electronic Engineering, University of Hong Kong, Pokfulam Road, Hong Kong

Martin L. Majewski
Department of Computer Science and Electrical Engineering, The University of Queensland, Brisbane Old 4072, Australia

(Received 3 September 1998; accepted for publication 6 January 1999)

An extension of the Adachi model with the adjustable broadening function, instead of the Lorentzian one, is employed to model the optical constants of GaP, InP, and InAs. Adjustable broadening is modeled by replacing the damping constant with the frequency-dependent expression. The improved flexibility of the model enables achieving an excellent agreement with the experimental data. The relative rms errors obtained for the refractive index equal 1.2% for GaP, 1.0% for InP, and 1.6% for InAs. © *1999 American Institute of Physics.* [S0021-8979(99)05807-7]

I. INTRODUCTION

Group III–V semiconductors are playing an increasingly important role in integrated optics because they offer the potential for the integration of sources, detectors, switches, and modulators. Experimental data on the optical constants as a function of energy are available for a number of III–V compounds.[1,2] However, the usefulness of the experimental data is limited by the fact that they are not expressed as analytical functions of photon energy and critical-point (CP) energies in the Brillouin zone. Therefore, it is necessary to model the experimental data with an analytical model. The model employed must also be simple and concise, and at the same time give a reasonably good approximation of the optical spectra of the investigated materials.

In modeling the optical constants of semiconductors, two approaches are frequently used: the standard critical-point (SCP) model[3,4] and the damped harmonic oscillator (DHO) model.[5,6] Both approaches are widely known to have limitations. The SCP model can accurately describe the second and third derivatives of the dielectric function and thus provide information about the positions of CPs (by fitting the SCP model to the second derivative of the experimental data), but it is inadequate for describing the dielectric function itself. On the other hand, the DHO model can describe the experimental dielectric function but not its derivatives. The DHO also requires a large number of adjustable parameters and is not directly related to the band structure, i.e., it cannot provide accurate information about CP energies.

Adachi's model dielectric function (MDF) (Refs. 7 and 8) represents a relatively simple model which combines the two aforementioned approaches with the addition of excitonic terms at the two lowest-energy gaps and their spin-orbit split counterparts. The MDF describes the dielectric function with terms attributed to the four energy gaps ($E_0, E_0+\Delta_0, E_1, E_1+\Delta_1$) and the damped harmonic oscillators describe the contributions from higher lying transitions [$E_0', E_2(X), E_2(\Sigma)$]. This model is not very accurate, however, and several modifications have been proposed recently.[9–18] Forouhi and Bloomer[19] have proposed a model which is also related to the band structure and requires fewer parameters (up to 14). However, for the materials investigated here, this model does not bring about significant improvement in accuracy over the conventional Adachi's model, especially around the fundamental band-gap E_0.

All the models mentioned above have a common shortcoming: they assume a Lorentzian broadening of the absorption line, which gives rise to higher absorption and poor accuracy around the fundamental absorption edge as a result of the extended wings of the Lorentzian function. The fact that Lorentzian broadening does not describe the optical spectrum accurately has already been recognized and discussed by several groups.[20–23] Rakić and Majewski[23] have shown that the Adachi model, with a Gaussian-like broadening function, can describe accurately the dispersion and absorption of GaAs and AlAs even in the vicinity of the E_0, where the original model of Ozaki and Adachi[9] is highly inaccurate. In this work, we use a similar model, which considers the contribution of exitonic terms only at E_0, $E_0+\Delta_0$ CPs, since the excitonic effects are usually more pronounced at E_0 than at any other CPs.[24] Furthermore, the

[a)]Electronic mail: ehli@eee.hku.hk

description of the contributions of a discrete series of two-dimensional Wannier excitons at E_1, $E_1+\Delta_1$ CPs in the MDF and its modifications[9,23] usually leads to an overestimation of the strength of these excitons as well as their binding energies.[25] In order to ensure that all the terms considered to be contributing to the dielectric function and all obtained parameters have physical justification, the model employed here differs from previous calculations of optical constants of these materials[10,11,17] with one additional degree of freedom. The contributions of indirect transitions are not taken into account here because they represent second-order perturbation. Therefore, their strength is significantly less than that of the direct transitions, while the Adachi model gives unreasonably high values for the strength of indirect transitions in order to improve the agreement with the experimental data in the region around the fundamental absorption edge.[17] It will be shown that our model, which includes the adjustable broadening function, can describe the experimental data in this region accurately. In the vicinity of the fundamental absorption edge, the broadening function in our model is Gaussian-like, enabling us to model the sharper structure present in the experimental data without artificially introducing additional terms to the description of the dielectric function.

In the following section, a description of the employed model is given. In Sec. III, the model parameters are determined and a discussion of the results obtained as compared with the previous ones is given. Finally, conclusions are drawn.

II. MODEL OF THE DIELECTRIC FUNCTION

We shall briefly describe the model applied for the dielectric function. The dielectric function in the Adachi model is represented by the sum of terms describing the transitions at the critical points in the joint density of states. In the modification proposed by Rakić and Majewski,[23] damping constants Γ_i are replaced with the frequency-dependent expression $\Gamma_i'(\omega)$.

A. E_0 and $E_0+\Delta_0$ transitions

Under the parabolic band assumption, the contributions of the three-dimensional M_0 CPs E_0 and $E_0+\Delta_0$ are given by[9]

$$\epsilon^{\mathrm{I}}(\omega)=AE_0^{-3/2}\left[f(\chi_0)+\frac{1}{2}\left(\frac{E_0}{E_0+\Delta_0}\right)^{3/2}f(\chi_{0s})\right], \tag{1}$$

where

$$f(y)=y^{-2}[2-(1+y)^{1/2}-(1-y)^{1/2}], \tag{2}$$

$$\chi_0=\frac{\hbar\omega+i\Gamma_0}{E_0}, \tag{3}$$

$$\chi_{0s}=\frac{\hbar\omega+i\Gamma_0}{E_0+\Delta_0}, \tag{4}$$

where A and Γ_0 are the strength and damping constants of the E_0 and $E_0+\Delta_0$ transitions, respectively. The contribution of the excitons (discrete series of exciton lines at the E_0 and $E_0+\Delta_0$ CPs) is given by[26]

$$\epsilon^{\mathrm{II}}(\omega)=\sum_{m=1}^{\infty}\frac{A_0^{ex}}{m^3}\frac{1}{E_0-(G_0/m^2)-E-i\Gamma_0}, \tag{5}$$

where A_0^{ex} is the strength and G_0 is the binding energy. A summation of the excitonic terms is performed until the contribution of the next term is less than 10^{-4}.

B. E_1 and $E_1+\Delta_1$ transitions

For the contributions of the two-dimensional M_0 CPs E_1 and $E_1+\Delta_1$, by taking the matrix element to be constant with respect to energy, Adachi[9] has obtained the following expression:

$$\epsilon^{\mathrm{III}}(\omega)=-B_1\chi_1^{-2}\ln(1-\chi_1^2)-B_{1s}\chi_{1s}^{-2}\ln(1-\chi_{1s}^2), \tag{6}$$

where

$$\chi_1=\frac{\hbar\omega+i\Gamma_1}{E_1}, \tag{7}$$

$$\chi_{1s}=\frac{\hbar\omega+i\Gamma_1}{E_1+\Delta_1}, \tag{8}$$

and $B_1(B_{1s})$ and Γ_1 are the strength and the damping constants of the E_1 and $E_1+\Delta_1$ transitions, respectively.

C. E_0', $E_2(X)$, and $E_2(\Sigma)$ transitions

The origin of the transitions E_0', $E_2(X)$, and $E_2(\Sigma)$ is not completely clear, since they do not correspond to a single, well-defined CP. However, these features can be adequately modeled with damped harmonic oscillators,[9] which are characterized by energy E_j, oscillator strength $f_j=\sqrt{C_jE_j^2}$, and damping constant Γ_j, $j=2,3,4$:

$$\epsilon^{\mathrm{IV}}(\omega)=\sum_{j=2}^{4}\frac{f_j^2}{E_j^2-(\hbar\omega)^2-i\hbar\omega\Gamma_j}. \tag{9}$$

D. The frequency-dependent damping

The damping constants in Eqs. (1)–(9) are replaced with[20,23]

$$\Gamma_i'(\omega)=\Gamma_i\exp\left[-\alpha_i\left(\frac{\hbar\omega-E_i}{\Gamma_i}\right)^2\right]. \tag{10}$$

In this way, the shape of the line varies with the ratio of parameters α_j and Γ_j. The line shapes vary from purely Lorentzian (for $\alpha=0$) to nearly Gaussian ($\alpha=0.3$) profiles. For large α_j/Γ_j ratios, the wings of the peak in the imaginary part of the dielectric function $\epsilon_2(\omega)$ are even lower, thus enabling the elimination of extended absorption tails in ϵ_2, which is the signature of the Lorentzian line shapes. Since no broadening mechanism is set *a priori* (both α_j and Γ_j are adjustable model parameters), this model becomes very flexible.

E. Complete model for the dielectric function

The dielectric function is obtained by summing up the contributions of all the critical points described above, with Γ replaced by $\Gamma'(\omega)$:

$$\epsilon(\omega)=\epsilon_\infty+\epsilon^{\mathrm{I}}(\omega)+\epsilon^{\mathrm{II}}(\omega)+\epsilon^{\mathrm{III}}(\omega)+\epsilon^{\mathrm{IV}}(\omega), \tag{11}$$

where ϵ_∞ is the dielectric constant containing the contributions of the higher-lying transitions.

III. RESULTS AND DISCUSSION

To fit the model to the experimental data, we used the following objective function:

$$F=\sum_{i=1}^{i=N_p}\left[\left|\frac{\epsilon_1(\omega_i)-\epsilon_1^{\mathrm{expt}}(\omega_i)}{\epsilon_1^{\mathrm{expt}}(\omega_i)}\right|+\left|\frac{\epsilon_2(\omega_i)-\epsilon_2^{\mathrm{expt}}(\omega_i)}{\epsilon_2^{\mathrm{expt}}(\omega_i)}\right|\right]^2, \tag{12}$$

where N_p is the number of experimental points and $\epsilon_1(\omega_i)$, $\epsilon_2(\omega_i)$ are the calculated values of the real and the imaginary parts of the dielectric constant at frequency ω_i, while $\epsilon_1^{\mathrm{expt}}(\omega_i)$ and $\epsilon_2^{\mathrm{expt}}(\omega_i)$ are the corresponding experimental values. This objective function is chosen because it enables the minimization of discrepancies between the calculated and experimental data for both the real and imaginary parts of the dielectric function at the same time. The minimization of only one (real or imaginary) part of the dielectric function can lead to the deterioration in the accuracy of the estimated parameter values. Other objective functions (such as the sum of the squared relative errors instead of the squared sum of the absolute values of the relative errors) give similar results as the one employed here. The experimental values used in the determination of model parameters are tabulated from the *Handbook of Optical Constants of Solids I*.[1] The objective function is minimized with acceptance-probability-controlled simulated annealing algorithm with the adaptive move-generation procedure, which is described in detail in Refs. 27 and 28. The model parameter values obtained for all three materials are given in Table I. From the ratio of the parameters α_0 and Γ_0 in all cases, it can be concluded that the broadening function for the E_0 transition is very narrow, which is the principal reason why models involving the Lorentzian broadening (whose inherent characteristics are the extended wings of the broadening function) in this region are inaccurate. The critical-point energies obtained from our calculations are generally in good agreement with previous results.[29–31]

Figure 1 shows the real and imaginary parts of the index of refraction of GaP as a function of energy. The experimental data are represented with open circles; the solid line represents our calculations, the dotted line represents the results of Adachi,[11] and the dashed line represents the calculations of Forouhi and Bloomer.[19] The refractive index rms error obtained for our model is 1.2%, compared with the values of 13.6% for Adachi's MDF and 5.8% for the model of Forouhi and Bloomer. The conventional Adachi model gives the poorest agreement with the experimental data. Agreement with experiment is better for the calculations of Forouhi and Bloomer.[19] However, it can be observed that this model fails to describe accurately the optical properties of GaP below and around the fundamental band-gap E_0. The discrepancy present at the end of the investigated spectral range is probably due to the fact that data for energies higher than 5.5 eV are not taken into account on the determination of the model parameters.

TABLE I. Model parameter values.

Parameter	GaP	InP	InAs
ϵ_∞	0.111	0.500	1.142
A eV$^{1.5}$	13.381	4.062	3.264
Γ_0 eV	0.030	0.036	0.165
α_0	3.691	3.739	4.111
B_1 eV	2.393	2.946	2.704
B_{1s} eV	2.350	2.476	2.765
E_0 eV	2.734	1.346	0.450
$E_0+\Delta_0$ eV	2.811	1.425	0.870
Γ_1 eV	0.309	5.217	4.394
α_1	0.223	0.091	0.027
f_2 eV	5.162	5.997	3.984
Γ_2 eV	0.401	0.489	0.619
α_2	0.399	0.021	0.033
E_2 eV	5.125	4.742	2.639
f_3 eV	5.350	3.589	6.245
Γ_3 eV	0.508	0.414	0.542
α_3	0.011	0.029	0.008
E_3 eV	4.802	3.202	4.478
f_4 eV	3.695	3.627	3.312
Γ_4 eV	0.336	0.161	0.913
α_4	0.047	0.039	0.048
E_4 eV	3.643	6.800	6.217
A_0^{ex} eV	0.0001	0.0001	0.0003
G_0 eV	0.005	0.001	0.017
E_1 eV	3.666	3.100	2.650
$E_1+\Delta_1$ eV	3.632	3.120	2.665

The real and imaginary parts of the index of refraction of InP as a function of energy are shown in Fig. 2. The experimental data are represented by open circles; the solid line represents our calculations, the dotted line represents the results of Adachi,[11] and the dashed line represents the calcula-

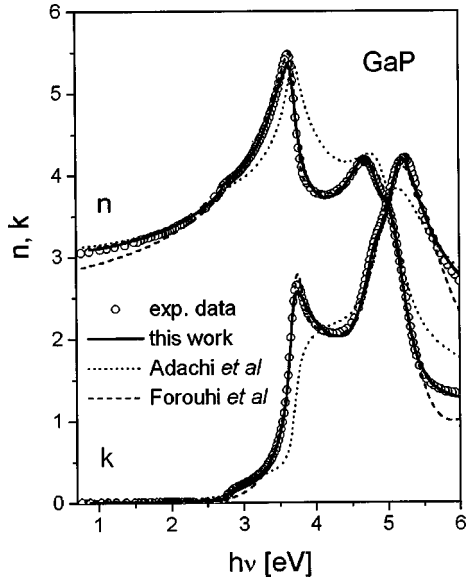

FIG. 1. The real and imaginary parts of the index of refraction for GaP as a function of energy: circles, experimental data; solid line, this work; dotted line, Adachi (see Ref. 11); and dashed line, Forouhi and Bloomer (see Ref. 19).

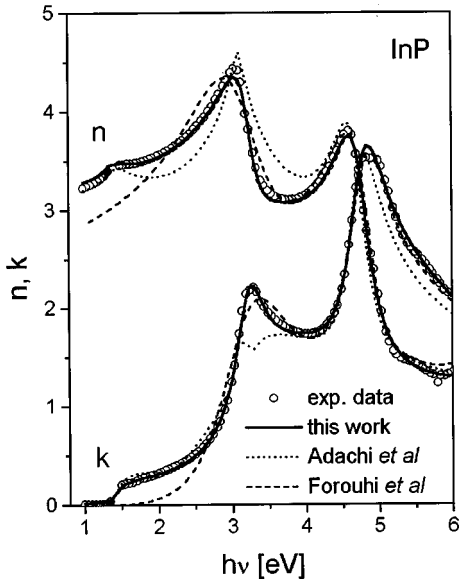

FIG. 2. The real and imaginary parts of the index of refraction for InP as a function of energy: circles, experimental data; solid line, this work; dotted line, Adachi (see Ref. 11); and dashed line, Forouhi and Bloomer (see Ref. 19).

tions of Forouhi and Bloomer.[19] For this material, we can make similar observations for GaP. The relative rms errors obtained for the refractive index are 1.0% for our calculations, 6.2% for Adachi's MDF, and 6.4% for the model of Forouhi and Bloomer.

Figure 3 depicts the real and imaginary parts of the index of refraction of InAs versus energy. The experimental data are represented by open circles; the solid line represents our calculations, the dotted line represents the results of Adachi,[11] and the dashed line represents the calculations of Forouhi and Bloomer.[19] For InAs, we obtain 1.6% relative rms error for the refractive index, while errors for the calculations of Adachi[11] and Forouhi and Bloomer[19] equal 6.5% and 2.3%, respectively. In this case, the results of Forouhi and Bloomer[19] are comparable to ours, i.e., their calculations give a rms error at 1.5 times higher than ours. The reason is that the available experimental data are above the band gap of this material, hence, inaccuracy is inevitable. However, when the fundamental absorption edge is within the investigated spectral region, as in the case of GaP and InP, our model is clearly superior to the other two, due to its adjustable broadening feature.

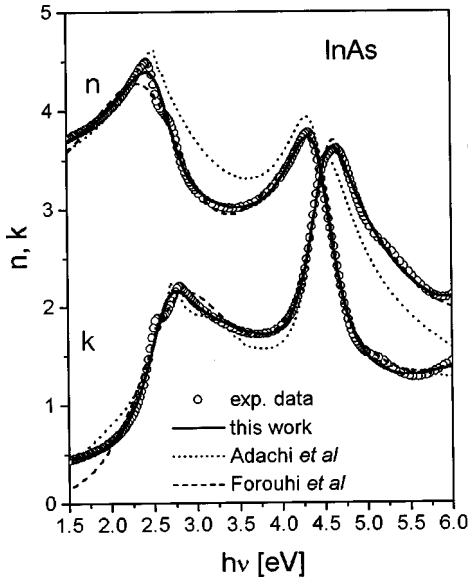

FIG. 3. The real and imaginary parts of the index of refraction for InAs as a function of energy: circles, experimental data; solid line, this work; dotted line, Adachi (see Ref. 11); and dashed line, Forouhi and Bloomer (see Ref. 19).

IV. CONCLUSION

We have modeled the optical constants of GaP, InP, and InAs in the spectral range from 1 to 6 eV. The calculation employed here is based on a simple and yet accurate model of optical constants. The great flexibility of the model resulting from an adjustable broadening mechanism (accomplished by frequency-dependent damping) enables one to achieve good agreement with the experimental data in a wide spectral range. Excellent agreement with the experimental data for all three investigated materials is obtained. The refractive index relative rms errors are 1.2%, 1.0%, and 1.6% for GaP, InP, and InAs, respectively. To the best of our knowledge, these should be the lowest errors obtained so far in the literature.

ACKNOWLEDGMENTS

This work is supported by the Research Grant Council (RGC) Earmarked Grant of Hong Kong. One of the authors (A.B.D.) acknowledges the support of a William Mong Postdoctoral Fellowship of the Faculty of Engineering for this work.

[1] *Handbook of Optical Constants of Solids I*, edited by E. D. Palik (Academic, Orlando, FL, 1985).
[2] *Handbook of Optical Constants of Solids II*, edited by E. D. Palik (Academic, San Diego, CA, 1991).
[3] M. Cardona, *Modulation Spectroscopy* (Academic, New York, 1969).
[4] D. E. Aspnes, in *Handbook on Semiconductors*, edited by M. Balkanski (North-Holland, Amsterdam, 1980), Vol. 2, p. 109.
[5] M. Erman, J. B. Theeten, P. Chambon, S. M. Kelso, and D. E. Aspnes, J. Appl. Phys. **56**, 2664 (1984).
[6] F. L. Terry, Jr., J. Appl. Phys. **70**, 409 (1991).
[7] S. Adachi, J. Appl. Phys. **53**, 5863 (1982).
[8] S. Adachi, J. Appl. Phys. **58**, R1 (1985).
[9] S. Ozaki and S. Adachi, J. Appl. Phys. **78**, 3380 (1995).
[10] S. Adachi, Phys. Rev. B **39**, 12612 (1989).
[11] S. Adachi, J. Appl. Phys. **66**, 6030 (1989).
[12] D. W. Jenkins, J. Appl. Phys. **68**, 1848 (1990).
[13] S. Adachi, T. Kimura, and N. Suzuki, J. Appl. Phys. **74**, 3435 (1993).
[14] R. J. Deri and M. A. Emanuel, J. Appl. Phys. **74**, 3435 (1993).
[15] Y. Kokubo and I. Ohto, J. Appl. Phys. **81**, 2042 (1997).
[16] J. Zheng, C.-H. Lin, and C. H. Kuo, J. Appl. Phys. **82**, 792 (1997).
[17] S. Adachi, Phys. Rev. B **41**, 3504 (1990).
[18] T. Aoki and S. Adachi, J. Appl. Phys. **69**, 1574 (1991).
[19] A. R. Forouhi and I. Bloomer, Phys. Rev. B **38**, 1865 (1988).
[20] C. C. Kim, J. W. Garland, H. Abad, and P. M. Raccah, Phys. Rev. B **45**, 11749 (1992).
[21] O. Stenzel, R. Petrich, W. Scharff, A. Tikhonravov, and V. Hopfe, Thin Solid Films **207**, 324 (1992).
[22] A. Franke, A. Stendal, O. Stenzel, and C. von Borczyskowski, Pure Appl. Opt. **5**, 845 (1996).

[23] A. D. Rakić and M. L. Majewski, J. Appl. Phys. **80**, 5909 (1996).
[24] C. C. Kim and S. Sivananthan, J. Appl. Phys. **78**, 4003 (1995).
[25] C. Tanguy, IEEE J. Quantum Electron. **32**, 1746 (1996).
[26] S. Adachi, Phys. Rev. B **41**, 1003 (1990).
[27] A. D. Rakić, J. M. Elazar, and A. B. Djurišić, Phys. Rev. E **52**, 6862 (1995).
[28] A. B. Djurišić, A. D. Rakić, and J. M. Elazar, Phys. Rev. E **55**, 4797 (1997).
[29] S. Adachi, *Physical Properties of III–V Semiconductor Compounds. InP, InAs, GaAs, GaP, InGaAs and InGaAsP* (Wiley, New York, 1992).
[30] M. Cardona, J. Appl. Phys. **32**, 2151 (1961).
[31] D. E. Aspnes and A. A. Studna, Phys. Rev. B **27**, 985 (1983).